Uplift and magma intrusion at Long Valley caldera from InSAR and gravity measurements

Pietro Tizzani[1], Maurizio Battaglia[2], Giovanni Zeni[3], Simone Atzori[4], Paolo Berardino[5], Riccardo Lanari[5]

[1]Consiglio Nazionale delle Ricerche (CNR) Istituto per il Rilevamento Elettromagnetico dell'Ambiente, Via Diocleziano 324, 80124 Naples, Italy, and Istituto Nazionale di Geofisica e Vulcanologia–Osservatorio Vesuviano, Via Diocleziano 324, 80124 Naples, Italy

[2]Department of Earth Sciences, University of Rome "La Sapienza," Piazzale A. Moro 5, 00185 Rome, Italy, and U.S. Geological Survey, Volcano Hazards Team, Menlo Park, California 94025, USA

[3]CNR Istituto per il Rilevamento Elettromagnetico dell'Ambiente, Via Diocleziano 324, 80124 Naples, Italy, and Università degli Studi della Basilicata, Via dell'Ateneo Lucano 10, 85100 Potenza, Italy

[4]Istituto Nazionale di Geofisica e Vulcanologia–Centro Nazionale Terremoti, Via di Vigna Murata 605, 00143 Rome, Italy

[5]Consiglio Nazionale delle Ricerche (CNR) Istituto per il Rilevamento Elettromagnetico dell'Ambiente, Via Diocleziano 324, 80124 Naples, Italy

ABSTRACT

The Long Valley caldera (California) formed ~760,000 yr ago following the massive eruption of the Bishop Tuff. Postcaldera volcanism in the Long Valley volcanic field includes lava domes as young as 650 yr. The recent geological unrest is characterized by uplift of the resurgent dome in the central section of the caldera (75 cm in the past 33 yr) and earthquake activity followed by periods of relative quiescence. Since the spring of 1998, the caldera has been in a state of low activity. The cause of unrest is still debated, and hypotheses range from hybrid sources (e.g., magma with a high percentage of volatiles) to hydrothermal fluid intrusion. Here, we present observations of surface deformation in the Long Valley region based on differential synthetic aperture radar interferometry (InSAR), leveling, global positioning system (GPS), two-color electronic distance meter (EDM), and microgravity data. Thanks to the joint application of InSAR and microgravity data, we are able to unambiguously determine that magma is the cause of unrest.

INTRODUCTION

Interpreting geodetic measurements is particularly difficult in the case of slow, years-to-decades deformation such as that commonly observed at large Quaternary silicic calderas. For instance, Campi Flegrei caldera (Italy) experienced 3 m of uplift between 1969 and 1984, followed by slow subsidence since 1985 (De Natale et al., 2006). Yellowstone caldera has shown an even more complex behavior: uplift of resurgent domes within the caldera started sometime after 1923, reaching a total of 90 cm, but in 1984 the deformation reversed to subsidence at a rate of 1–2 cm/yr until 1992 (Dzurisin et al., 1994). Starting in 1992, the deformation began migrating from one resurgent dome to the other. Evidence from geodetic surveys suggests that magma intrusion and/or pressurization of magmatic volatiles may both drive uplift at Yellowstone (Chang et al., 2007). Independent observations such as microgravity changes over time, which are capable of resolving mass and density variations in the subsurface, may enable us to discriminate among the contributions of different mechanisms of unrest.

Geodetic measurements at Long Valley caldera (Fig. 1) from 1975 to 2007 using precise leveling, global positioning system (GPS), and two-color electronic distance meter (EDM) have revealed multiple episodes of caldera uplift centered at its resurgent dome (Hill, 2006). The fact that the resurgent dome uplift (Fig. 2) is much larger than that which can explained by seismic activity within and around the caldera, together with the observation that the onset of accelerated deformation precedes increases in earthquake activity by several weeks, suggests that the major source of caldera unrest is probably mass intrusion beneath the resurgent dome (Hill, 2006). Most of the deformation within the caldera can be modeled by a volumetric source with the geometry of a near-vertical pipe at a depth between 5 and 8 km, together with slip along faults in the caldera's south moat (Langbein, 2003). Previous results from repeated microgravity measurements have indicated a mass increase beneath the resurgent dome with a density in the range of 1180–2330 kg/m^3. On the basis of the relatively low density, this mass was interpreted to be a combination of magma and a gas-rich hydrothermal fluid (Battaglia et al., 2003). On the other hand, recent numerical work by Hurwitz et al. (2007) suggests that small differences in the values of host-rock permeability and anisotropy, the depth and rate of hydrothermal injection, and the value of the shear modulus may lead to significant variations in the magnitude, rate, and geometry of ground surface displacement. Compared to previous work

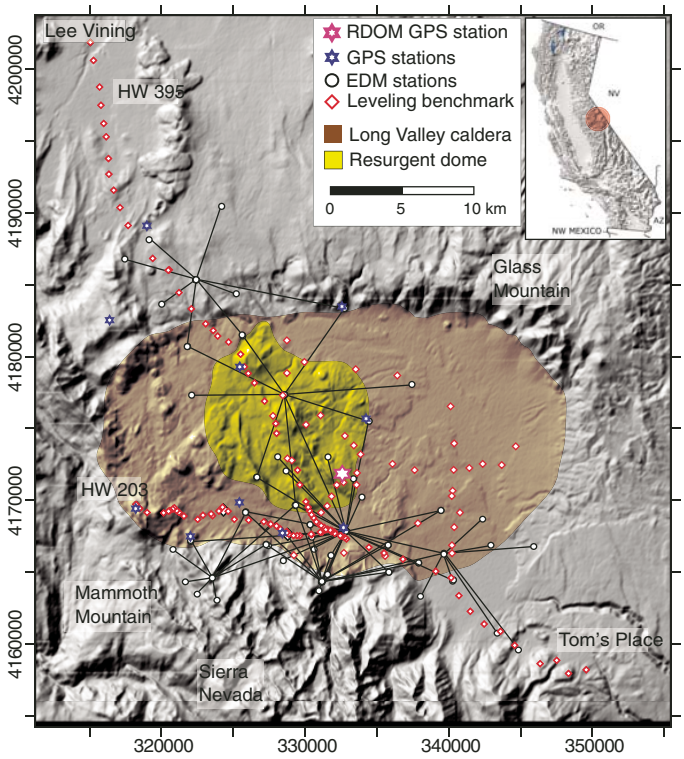

Figure 1. Shaded relief map of Long Valley caldera and monitoring sites. Brown—caldera; yellow—resurgent dome. Coordinates are in UTM NAD27. Inset in upper right corner shows location of study area. EDM—two-color electronic distance meter; GPS—global positioning system.

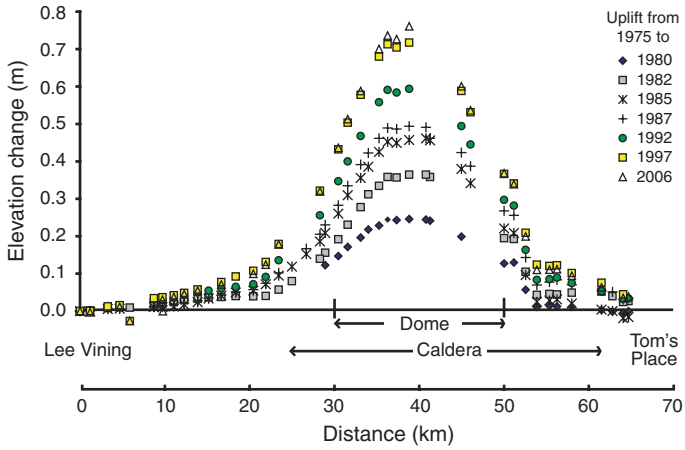

Figure 2. Vertical deformation along Highway 395 leveling route (Fig. 1). This route runs across Long Valley caldera resurgent dome. Symbols correspond to elevation differences from 1975 for specified time intervals (Dzurisin, Cascades Volcano Observatory, 2008, personal commun.).

TABLE 1. BEST-FIT STATISTICS AND PARAMETERS

Data sets (1992–1999)		**Weight**	
SAR 1992–1999 (points)	12,678	0.5	
EDM 1992–1999 (baselines)	70	0.5	
Best-fit statistics			
Final cost (χ^2_ν)	1.34		
SAR data: RMS (cm)	0.90	Null solution: 7.8	
EDM data: RMS (cm)	2.06	Null solution: 7.2	
Best-fit parameters	**Value**	**Search interval**	**95% bounds**
Semi-major axis *a* (m)	969	10–3000	
Axis ratio *b/a*	0.660	0.000–1.000	0.56–0.84
Depth (km)	7.643	3.000–9.000	6.6–8.7
Strike angle (°)	216	0–360	196–302
Dip angle (°)	63	0–90	30–77
Source center E (UTM)	332764	330000–336000	
Source center W (UTM)	4172754	4169000–4173000	
Volume change (km^3)	0.068	10^{-4}–0.800	

Note: SAR—synthetic aperture radar; EDM—two-color electronic distance meter; RMS—root mean square.

(e.g., Fialko et al., 2001; Battaglia et al., 2003), here we (1) determine the uplift using differential synthetic aperture radar interferometry (InSAR) deformation time series from 1992 to 2000; (2) increase the number of two-color EDM baselines to better constrain the source geometry; and (3) we do not assume a vertical prolate spheroid model. As a result, we are able to better constrain the geometry of the deformation source and obtain a more robust estimate of its density.

OBSERVATIONS

To measure the deformation of the entire caldera floor and its surroundings, we analyzed a data set composed of 21 descending orbit SAR images (track 485, frame 2845), acquired by the European Space Agency ERS-1/2 satellites, spanning the time interval from June 1992 to August 2000 (Tizzani et al., 2007). The ERS-1/2 satellite data were processed using the Small Baseline Subset (SBAS)–InSAR algorithm (Berardino et al., 2002), which allows us to detect surface displacements and analyze their temporal evolution by generating mean deformation velocity maps and time series projected along the radar line of sight (LOS). The InSAR measurements have a spatial resolution of ~100 m and an accuracy of ~2 mm/yr for the deformation velocity and ~10 mm for surface displacements. The InSAR results are consistent with the leveling and GPS measurements (Tizzani et al., 2007).

To minimize the influence from sources not related to the geological unrest, we selected for our analysis only those pixels for which the time series had a correlation greater than 0.95 with respect to the time series of the coherent SAR pixel closer (less than 100 m) to the permanent GPS station RDOM (U.S. Geological Survey [USGS] Earthquake Hazards Program [EHZ], 2008), which is located in the area of maximum uplift on the resurgent dome (Fig. 1).

In addition to the InSAR data, we included in our analysis leveling data from 1982 to 1999, two-color EDM data from 1992 to 2000 (U.S. Geological Survey, 2008), and gravity data from 1982 to 1999 (Battaglia et al., 2003). Given the time distribution of the available geodetic and gravity data sets and the need to have the largest possible signal-to-noise ratio, our modeling strategy was developed following a two-step approach. First, we inverted EDM and InSAR data from 1992 to 1999 to constrain the geometry of the source. We then used uplift and gravity changes between 1982 and 1999 to determine the density of that source (we assumed that the caldera deformation source remained constant from 1982 to 1999, which is justified by the symmetry, over the past 33 yr, of the displacement pattern measured along the leveling route that crosses the resurgent dome; Fig. 2).

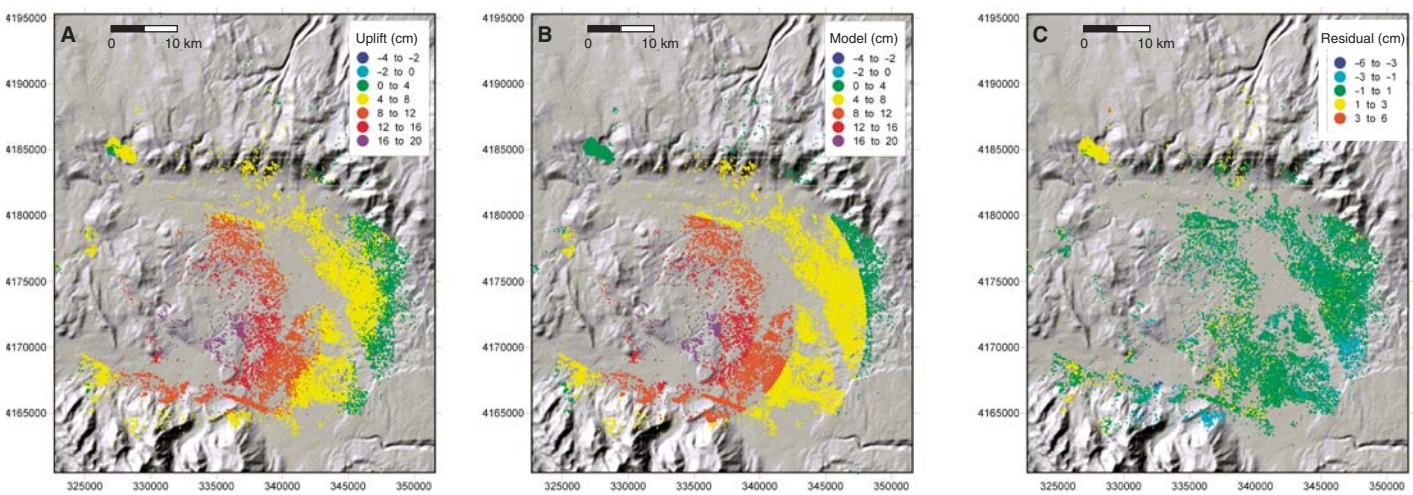

Figure 3. Modeling of deformation at Long Valley caldera by fitting a spheroidal source in an elastic homogeneous half space (see Table 1 for parameters). (A) 1992–1999 synthetic aperture radar interferometry (InSAR) data, (B) model, and (C) residual. We used a nonlinear inversion algorithm based on Levenberg-Marquardt least-squares approach (Levenberg, 1944; Marquardt, 1963). Coordinates are in UTM NAD27.

Previous modeling by Fialko et al. (2001), Battaglia et al. (2003), and Langbein (2003) has suggested that the intrusion beneath the resurgent dome is cigar-shaped. To uniquely determine the geometry of this cigar-shaped intrusion, we jointly inverted the EDM and InSAR data for a finite prolate spheroid in an elastic, homogeneous, isotropic half-space (Yang et al., 1988). We used a nonlinear inversion algorithm to determine the best-fit parameters for the spheroid. This algorithm is based on the Levenberg-Marquardt least-squares approach (Levenberg, 1944; Marquardt, 1963; Moré et al., 1980). Measurement errors are coded in the covariance matrix (Langbein, 2003; Tizzani et al., 2007). Given the large discrepancy between the number of EDM (70 baselines) and InSAR (~12,500 pixels) observations, but considering their complementary characteristics, we balanced their impact within the inversion algorithm by selecting a weighting such that the contribution of each data set to the model was the same (Table 1). Finally, we performed a statistical analysis to assess the impact of the data uncertainties on the model parameters (Parsons et al., 2006).

RESULTS AND CONCLUSIONS

The best-fitting source for the InSAR and EDM data is a tilted prolate spheroid (see Fig. 3; Table 1), the center of which is located beneath the resurgent dome at a depth between 6.6 and 8.7 km (95% confidence interval). The spheroid has a geometrical aspect ratio (ratio between the semi-minor and semi-major axis) of 0.56–0.84 (95% confidence interval). Our result confirms that the deformation source does not possess a spherical symmetry and is probably closer to a pipe-like body oriented southwest-northeast, with a strike angle (measured clockwise from north) between 196° and 302°. The spheroid is tilted 63° from the horizontal axis (95% confidence bounds are 30° to 77°).

We subsequently estimated the density of the intrusion by joint inversion (constrained by the source geometry determined previously) of the uplift and gravity measurements from 1982 to 1999. Gravity data are much noisier than geodetic data (Fig. 4A), but the 17 yr time span provides an excellent signal-to-noise ratio. The Long Valley gravity network was measured every summer from 1980 to 1985, abandoned for 14 yr, and then reoccupied in 1998 and 1999 (Jachens and Roberts, 1985; Battaglia et al., 2003). Most of the stations outside Long Valley caldera are on crystalline bedrock outcrops, while volcanic flows or sediments underlie the stations within the caldera. We measured the relative gravity at selected stations along closed loops starting from Tom's Place (Fig. 1). Data reduction included the removal of solid Earth tides and daily gravimeter drift. Finally, the measured relative gravity values were averaged using a least-squares method to obtain one gravity determination at each station (Battaglia et al., 2003). The average error (1 standard deviation) for the gravity surveys was ±8 μGal (Fig. 4A).

Before we could interpret the gravity changes over time, it was necessary to correct the gravity data for variation in the level of the water table, the free-air effect, and the deformation effect, due to the coupling between gravity and elastic deformation (e.g., Battaglia and Segall, 2004). The net effect of water table changes on the gravity measurements is small for the 1982–1999 interval, typically of the order of 10 μGal (Battaglia et al., 2003). We computed the free-air correction using the vertical displacement field derived by differencing the GPS-based and leveled orthometric

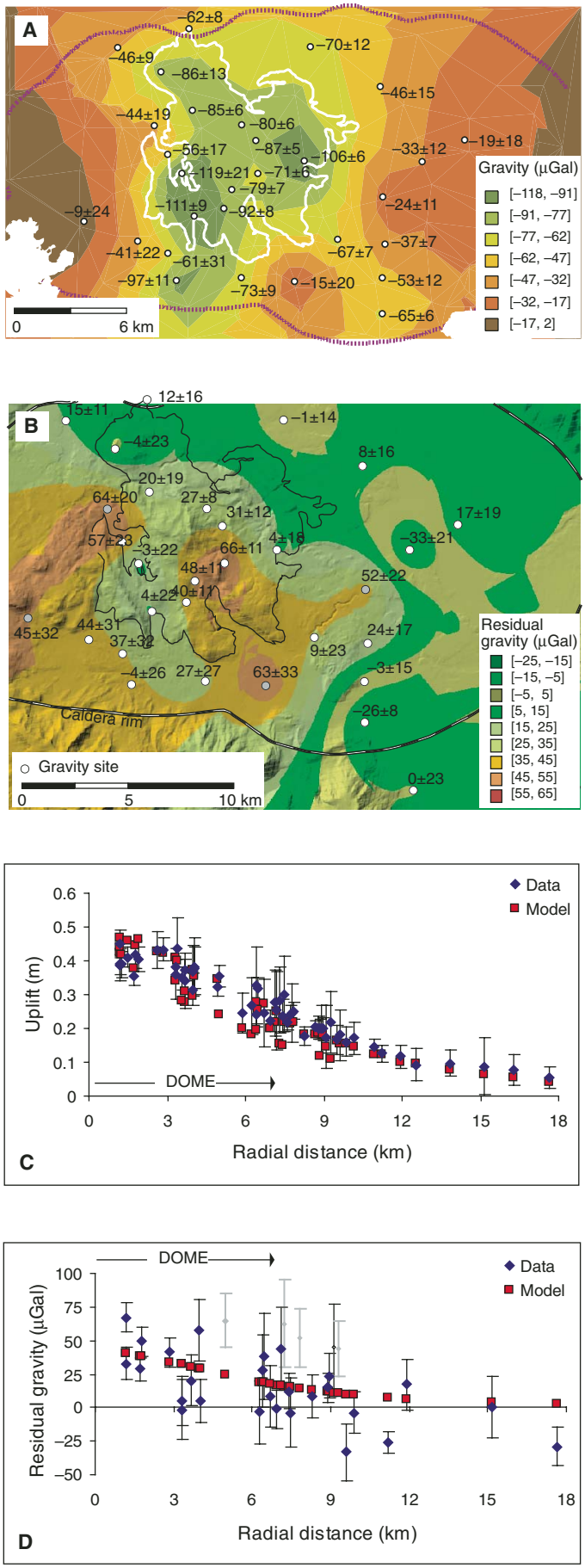

Figure 4. Modeling of deformation and gravity data. (A) Gravity changes between 1982 and 1999, modified after Battaglia et al. (2003); white line outlines resurgent dome. (B) Residual gravity changes between 1982 and 1999. Gray points show location of gravity sites that are located outside resurgent dome and have a significant anomaly. (C) Best-fit curve to vertical deformation (see Table 1 for spheroid parameters; error bars are 1 standard deviation). (D) Best-fit curve to residual gravity (see Table 1 for spheroid parameters; error bars are 1 standard deviation; Clark et al., 1986).

heights (Battaglia et al., 2008). Only 16 of the gravity stations coincided with a geodetic benchmark. We interpolated the uplift at the remaining stations by using kriging, a geostatistical interpolation technique (e.g., Goovaerts, 1997). The interpolation error was estimated through sequential Gaussian simulation (Battaglia et al., 2008). The deformation effect was not significant (e.g., Battaglia et al., 2006), with a maximum value of 1 μGal at sites on the resurgent dome.

The corrected gravity signal (residual gravity) depends only on the mass change accompanying the deformation (e.g., Eggers, 1987). The residual gravity (Fig. 4B) shows a positive anomaly centered on the resurgent dome with peak amplitude of 66 ± 11 μGal. The interpretation of the residual gravity anomaly is straightforward: a positive anomaly indicates that mass intruded into the crust, while a negative anomaly is a sign of a mass deficit. The positive residual gravity anomaly at Long Valley suggests mass intrusion into the crust beneath the resurgent dome. Most of the residual gravity values outside the resurgent dome are not significant at the 95% confidence level. The four sites with a significant anomaly outside the resurgent dome (Fig. 4B) are probably influenced by fluid intrusion beneath Mammoth Mountain (Foulger et al., 2003) and the caldera south moat (Prejean et al., 2002). Joint inversion of the deformation and residual gravity data gives a best-fit density of 2509 kg/m^3 for the intrusion (Figs. 4C and 4D). The 95% bootstrap bounds (Johnson, 2001) on density are 2192–3564 kg/m^3. These results suggest that inflation of the resurgent dome from 1982 through 1999 was the result of an intrusion of basaltic to silicic magma. Compared to previous studies (Battaglia et al., 2003), we better constrain the source of unrest thanks to the dense spatial coverage of deformation provided by InSAR. The new inversion algorithm allowed us to search for the best-fit spheroid without any geometrical assumptions (e.g., that the source is vertical). Given that the density of the intrusion is strongly dependent on its geometry, the robust bounds we found on the geometry provide stronger constraints on the density itself.

ACKNOWLEDGMENTS

The European Space Agency (ESA), P. Lundgren (Jet Propulsion Laboratory), A. Hooper (Nordic Volcanological Center), and M. Simons (Caltech) provided the ERS synthetic aperture radar (SAR) data through the WInSAR program. The caldera digital elevation model was acquired through the Shuttle Radar Topography Mission archive. The Technical University of Delft provided the precise ERS-1/2 satellite orbit state vectors. Thanks are also due to the Italian Gruppo Nazionale di Vulcanologia, Istituto Nazionale di Geofisica e Vulcanologia, which originally funded our InSAR study on Long Valley caldera. Comments by P. Lundgren, W. Chadwick, and M. Poland greatly helped to improve the manuscript.

REFERENCES CITED

Battaglia, M., and Segall, P., 2004, The interpretation of gravity changes and crustal deformation in active volcanic areas: Pure and Applied Geophysics, v. 161, p. 1453–1467, doi: 10.1007/s00024–004–2514–5.

Battaglia, M., Segall, P., and Roberts, C.W., 2003, The mechanics of unrest at Long Valley caldera, California. 2. Constraining the nature of the source using geodetic and micro-gravity data: Journal of Volcanology and Geothermal Research, v. 127, p. 219–245, doi: 10.1016/S0377–0273(03)00171–9.

Battaglia, M., Troise, C., Obrizzo, F., Pingue, F., and De Natale, G., 2006, Evidence for fluid migration as the cause of unrest at Campi Flegrei caldera (Italy): Geophysical Research Letters, v. 33, doi: 10.1029/2005GL024904.

Battaglia, M., Dzurisin, D., Langbein, J., Svarc, J., and Hill, D.P., 2008, Converting NAD83 GPS Heights into NAVD88 Elevations with LVGEOID, a Hybrid Geoid Height Model for the Long Valley Volcanic Region, California: U.S. Geological Survey Scientific Investigation Report 2007–5255, 32 p.

Berardino, P., Fornaro, G., Lanari, R., and Sansosti, E., 2002, A new algorithm for surface deformation monitoring based on small baseline differential SAR interferograms: IEEE Transactions on Geoscience and Remote Sensing, v. 40, p. 2375–2383, doi: 10.1109/TGRS.2002.803792.

Chang, W.L., Smith, R.B., Wicks, C., Farrell, J.M., and Puskas, C.M., 2007, Accelerated uplift and magmatic intrusion of the Yellowstone caldera, 2004–2006: Science, v. 318, doi: 10.1126/science.1146842.

Clark, D.A., Saul, S.J., and Emerson, D.W., 1986, Magnetic and gravity anomalies of a triaxial ellipsoid: Exploration Geophysics, v. 17, p. 189–200, doi: 10.1071/EG986189.

De Natale, G., Troise, C., Pingue, F., Mastrolorenzo, G., Pappalardo, L., Battaglia, M., and Boschi, E., 2006, The Campi Flegrei caldera: Unrest mechanisms and hazard, *in* De Natale, G., et al, eds., Mechanisms of Activity and Unrest at Large Calderas: Geological Society of London Special Publication 269, p. 25–45.

Dzurisin, D., Yamashita, K.M., and Kleinman, J.W., 1994, Mechanisms of crustal uplift and subsidence at the Yellowstone caldera, Wyoming: Bulletin of Volcanology, v. 56, p. 261–270.

Eggers, A., 1987, Residual gravity changes and eruption magnitudes: Journal of Volcanology and Geothermal Research, v. 33, p. 201–216, doi: 10.1016/0377–0273(87)90062-X.

Fialko, Y., Simons, M., and Khazan, Y., 2001, Finite source modelling of magmatic unrest in Socorro, New Mexico, and Long Valley, California: Geophysical Journal International, v. 146, p. 191–200.

Foulger, G.R., Julian, B.R., Pitt, A.M., Hill, D.P., Malin, P.E., and Shalev, E., 2003, Three-dimensional crustal structure of Long Valley caldera, California, and evidence for the migration of CO_2 under Mammoth Mountain: Journal of Geophysical Research, v. 108, doi: 10.1029/2000JB000041.

Goovaerts, P., 1997, Geostatistics for Natural Resources Evaluation: New York, Oxford University Press, 480 p.

Hill, D.P., 2006, Unrest in Long Valley caldera, California, 1978–2004, *in* De Natale, G., et al., eds., Mechanisms of Activity and Unrest at Large Calderas: Geological Society of London Special Publication 269, p. 1–24.

Hurwitz, S., Christiansen, L.B., and Hsieh, P.A., 2007, Hydrothermal fluid flow and deformation in large calderas: Inferences from numerical simulations: Journal of Geophysical Research, v. 112, doi: 10.1029/2006JB004689.

Jachens, R., and Roberts, C., 1985, Temporal and areal gravity investigations at Long Valley caldera, California: Journal of Geophysical Research, v. 90, p. 11,210–11,218, doi: 10.1029/JB090iB13p11210.

Johnson, R.W., 2001, An introduction to the bootstrap: Teaching Statistics, v. 23, p. 49–54, doi: 10.1111/1467–9639.00050.

Langbein, J., 2003, Deformation of the Long Valley caldera, California: Inferences from measurements from 1988 to 2001: Journal of Volcanology and Geothermal Research, v. 127, p. 247–267, doi: 10.1016/S0377–0273(03)00172–0.

Levenberg, K., 1944, A method for the solution of certain non-linear problems in least squares: Quarterly Journal of Applied Mathematics, v. 2, p. 164–168.

Marquardt, D., 1963, An algorithm for least-squares estimation of nonlinear parameters: SIAM Journal of Applied Mathematics, v. 11, p. 431–441, doi: 10.1137/0111030.

Moré, J.J, Garbow, B.S., and Hillstrom, K. E., 1980, User Guide for MINPACK-1: Argonne National Laboratory Report ANL-80–74, 49 p.

Parsons, B., Wright, T., Rowe, P., Andrews, J., Jackson, J., Walker, R., Khatib, M., Talebian, M., Bergman, E., and Engdahl, E.R., 2006, The 1994 Sefidabeh (eastern Iran) earthquakes revisited: New evidence from satellite radar interferometry and carbonate dating about the growth of an active fold above a blind thrust fault: Geophysical Journal International, v. 164, p. 202–217, doi: 10.1111/j.1365–246X.2005.02655.x.

Prejean, S., Ellsworth, W., Zoback, M., and Waldhauser, F., 2002, Fault structure and kinematics of the Long Valley caldera region, California, revealed by high-accuracy earthquake hypocenters and focal mechanism stress inversions: Journal of Geophysical Research, v. 107, doi: 10.1029/2001JB001168.

Tizzani, P., Berardino, P., Casu, F., Euillades, P., Manzo, M., Ricciardi, G.P., Zeni, G., and Lanari, R., 2007, Surface deformation of Long Valley caldera and Mono Basin, California, investigated with the SBAS-InSAR approach: Remote Sensing of Environment, v. 108, p. 277–289, doi: 10.1016/j.rse.2006.11.015.

U.S. Geological Survey, 2008, Long Valley Volcano Observatory (LVO), EDM time series: http://lvo.wr.usgs.gov/monitoring/index.html#deformation (May 2008).

U.S. Geological Survey Earthquake Hazards Program (EHZ), 2008, RDOME time series: http://quake.usgs.gov/research/deformation/gps/auto/LongValley/rdom/index.html (May 2008).

Yang, X., Davis, P.M., and Dieterich, J.H., 1988, Deformation from inflation of a dipping finite prolate spheroid in an elastic half-space as a model for volcanic stressing: Journal of Geophysical Research, v. 93, p. 4249–4257, doi: 10.1029/JB093iB05p04249.

Manuscript received 2 July 2008
Revised manuscript received 15 September 2008
Manuscript accepted 20 September 2008

Printed in USA